Self-healing high-order harmonic generation from curved relativistic plasma mirrors with Bessel-Gaussian beams

Zeyue Pang, Peng Chen, and Zi-Yu Chen [*]

Key Laboratory of High Energy Density Physics and Technology (MoE), College of Physics, Sichuan University, Chengdu 610064, China

Coherent focusing of high-order harmonic generation (HHG) from optically curved relativistic plasma mirrors provides a promising route to achieve unprecedented high intensities, opening up prospects to study phenomena occurring in extremely strong fields, the region of which is however limited within extremely small spatial and temporal scales. Here through three-dimensional particle-in-cell simulations we demonstrate HHG driven by Bessel-Gaussian beams exhibiting the intriguing feature of self-healing up to the relativistic and extreme nonlinear regime. This allows a secondary intensification of reflected fields after the focus of curved plasma mirrors and thus extends the high-intensity region in both space and time, beneficial for extreme field applications.

I. INTRODUCTION

High-order harmonic generation (HHG) from relativistically intense laser-irradiated mirrorlike overdense plasma surfaces is an extreme nonlinear process that produces high-brightness coherent light sources with short wavelengths in the extreme ultraviolet to x-ray region and temporal duration in the attosecond regime [1]. The physical mechanism can be interpreted as spectral Doppler upshifting and temporal compression of laser pulses reflected from relativistically oscillating plasma mirrors [2–6], under the combined action of laser ponderomotive force and charge-separation electrostatic force. Considering a realistic laser pulse with transversely nonuniform (e.g., Gaussian) intensity distribution, the laser light pressure also induces an optically dented plasma surface that can serve as a curved plasma mirror to simultaneously focus the high-order harmonics [7].

The intensity of a light pulse at focus is $I = U/\tau A$, which is proportional to the pulse energy U and inversely proportional to the pulse duration τ and the focal spot area A that scales as λ^2, with λ being the wavelength. Since the high-order harmonics from relativistic plasma mirrors have wavelengths [6] and durations [8] much shorter than those of the driving laser pulse, in addition to a relatively slow decaying spectrum [4], the intensity of focused high-order harmonics can be boosted significantly, reaching unprecedented levels [9], far beyond what can be realized by current or near-term high-power laser facilities based on the chirped-pulse amplification technique. Therefore, HHG from relativistic plasma mirrors has been proposed as a promising route to achieve extreme light intensities [9–12], even approaching the Schwinger limit that characterizes the light intensity high enough to "break down" vacuum [9,13,14]. Such a novel route may open up possibilities to allow experimental access to study intriguing phenomena in the strong-field quantum electrodynamics (QED) regime [15].

Yet, immense challenges must be confronted before utilizing the extreme field sources based on coherently focused high-order harmonics by curved relativistic plasma mirrors to study physical processes of interest. One of the main issues is the extremely small size of the strong-field region, which is typically of the nanometer spatial scale around the focal point and lasts for a temporal scale of attoseconds. This makes experimental studies, such as externally injecting electrons or nuclei to the extreme intensity region and detecting their strong-field nonlinear QED dynamics [14], a formidable task.

In this work, we introduce Bessel beams instead of the conventional Gaussian beams as the driving lasers. Bessel beams are a propagation-invariant type of solution to the Helmholtz equation [16], which exhibit unusual properties such as a high degree of resistance to diffraction and self-healing their spatiotemporal profiles after distortions by obstacles [17,18]. As such, Bessel beams have gathered attention in enormous applications, with experimental demonstrations ranging from extended depth-of-focus imaging [19] to long-distance underwater optical transmission [20] to material processing [21] to HHG in gas targets [22].

Through three-dimensional (3D) particle-in-cell (PIC) simulations, we show that high-order harmonics driven by Bessel light beams can inherit the self-healing feature of the driving pulse albeit in the relativistic and extreme nonlinear regime. In contrast to standard Gaussian laser-driven high-order harmonics from curved relativistic plasma mirrors, which only reach a peak intensity at the focus and then quickly diverge to low intensity once the focal point is passed, high-order harmonics driven by Bessel beams can gradually be restored to a transverse Bessel-like intensity distribution even after diverging from the focal point of the curved plasma mirrors. This allows the high-order harmonics to form a secondary focusing process, which tends to preserve the high intensity for a longer time. The novel features of harmonic self-healing and refocusing can extend the high-intensity region in both space and time.
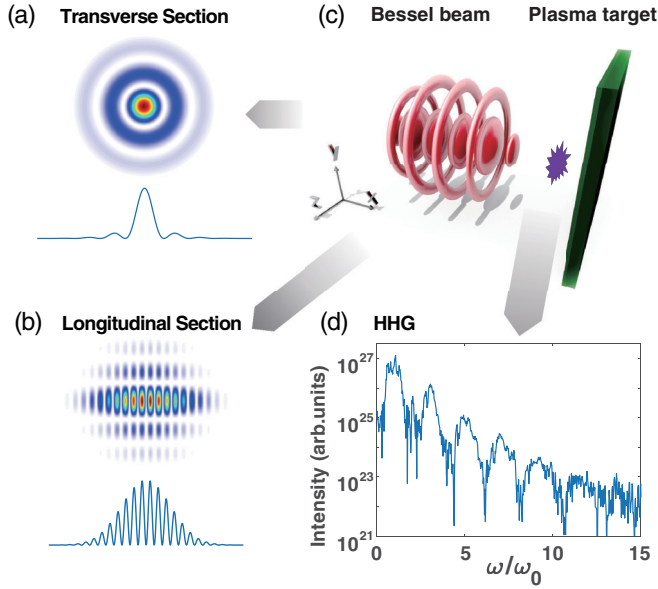
─────────
[*]ziyuch@scu.edu.cn

FIG. 1. High-order harmonic generation from Bessel-Gaussian-beam-driven relativistic plasma mirrors. (a) Transverse intensity profile of the Bessel-Gaussian beam described by a zeroth-order Bessel function of the first kind with a Gaussian envelope to ensure finite energy. (b) Longitudinal intensity profile exhibiting a Gaussian envelope. (c) Sketch of the simulation setup, where a Bessel-Gaussian beam is normally incident on a plasma slab target. (d) Typical high-order harmonic spectrum obtained by a 1D line cut of 2D spatial Fourier transform of the reflected field in the $z = 0$ plane at $t = 21T_0$.

II. SIMULATION SETUP

The 3D PIC simulations are performed using the VLPL (Virtual Laser Plasma Lab) code [23]. The driving Bessel pulse is polarized in the y direction and propagates along the x axis with a wavelength of $\lambda_0 = 800$ nm. The initial electric field of the Bessel pulse can be described as [16,24]

$$E = a_0 J_0\left(\frac{r}{r_0}\right) \exp\left(\frac{-r^2}{2w_0^2}\right) \exp\left(\frac{-t^2}{2t_0^2}\right) \exp[i(k_0 x - \omega_0 t)],$$

(1)

where $a_0 = eA_0/m_e c^2 = 15$ is the normalized laser vector potential, A_0 is the vector potential, ω_0 and k_0 are the laser angular frequency and wave number, e is the elementary charge, m_e is the electron mass, c is the light speed in vacuum, $J_0(r/r_0)$ is the zeroth-order Bessel function of the first kind with $r = \sqrt{y^2 + z^2}$ being the radial distance in the $y - z$ plane and $r_0 = 1.2\lambda_0$ approximately the full width at half maximum (FWHM) of the central peak, $\exp(-r^2/2w_0^2)$ with $w_0 = 6.86\lambda_0$ is a transverse Gaussian envelope to ensure finite energy of the Bessel beam and thus such a pulse is called a Bessel-Gaussian beam [24] [see Fig. 1(a) for the transversely spatial intensity profile], $\exp(-t^2/2t_0^2)$ with $t_0 = 2.12T_0$ indicates the temporal profile is Gaussian with a FWHM duration of $\tau_0 = 2\sqrt{2 \ln 2}\, t_0 \approx 5T_0$ [see Fig. 1(b) for the longitudinally temporal intensity distribution], and $T_0 \approx 2.67$ fs is the laser period. In practice, the intense Bessel-Gaussian beam can be generated through reflecting a normal Gaussian laser

beam off a conical mirror as experimentally demonstrated in Refs. [25,26] and then focusing it to high intensity [27].

We consider the Bessel-Gaussian beam normally incident on a fully ionized plasma slab target for the sake of simplicity, as shown schematically in Fig. 1(c). The plasma slab has a density of $n_0 = 5n_c$ and a thickness of $4\lambda_0$. Here, $n_c = m_e \omega_0^2/4\pi e^2$ is the critical plasma density with respect to the fundamental laser frequency ω_0. The plasma slab front surface is located at $x = 39\lambda_0$. Ions are assumed to be immobile in the simulations due to the short pulse duration.

The 3D simulations have a box size of $X \times Y \times Z = 46\lambda_0 \times 32\lambda_0 \times 32\lambda_0$. The grid step size is $\lambda_0/50$ in the x direction and $\lambda_0/20$ in both the y and z directions. The time step is $0.0173T_0$. Each cell is filled with eight macroparticles. Both fields and particles are subjected to absorbing boundary conditions to avoid artificial reflections. The technique of a perfectly matched layer with a width of $1\lambda_0$ is used to effectively damp the fields at boundaries to far below the relativistic threshold.

III. RESULTS AND DISCUSSION

Upon reflection from the relativistically oscillating plasma mirrors, phase modulation is imposed on the incident Bessel-Gaussian beams, and thus the reflected field contains high-order harmonic components in the frequency domain. Figure 1(d) shows a typical 1D high-order harmonic spectrum obtained through a line cut of 2D spatial Fourier transform of the reflected field in the $x - y$ ($z = 0$) plane at $t = 21T_0$. Clear harmonic structure is observed up to about the 11th order, limited by the spatial resolution of the 3D simulations. Only odd-order harmonics are generated, as the laser is at normal incidence [3].

During the laser-plasma interactions, due to the intense laser light pressure, the initially flat plasma surface is pushed inwards and exhibits curved plasma mirrors, as shown in gray scale in Fig. 2. The plasma-mirror denting parameter induced
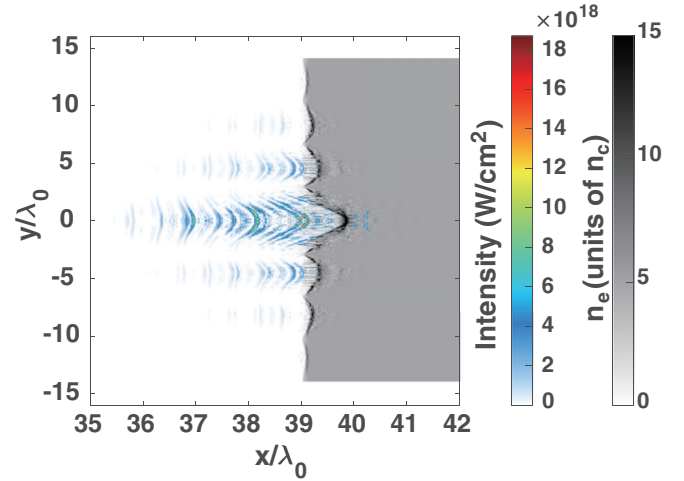

FIG. 2. Focusing of high-order harmonics by curved plasma mirrors generated by laser radiation pressure-induced plasma surface denting at $t = 6T_0$. The gray scale map represents the plasma electron density, while the color map displays the high-order harmonic fields with harmonic order $n \geqslant 3$.

by the main peak is $\delta_T \approx 0.5\lambda_0$, which is defined as the difference between the position $x_e|_{y=0}$ of the plasma-mirror surface at $y = 0$ (center of the focal spot) and its position $x_e|_{y=\sqrt{2}w_0}$ at $y = \sqrt{2}w_e$ ($w_e = 2\lambda_0$ is the half spatial width at $1/e$ of the laser-field amplitude) [28]. The light fields, including the generated high-order harmonic components, reflected by the curved plasma mirrors thus tend to have curved wave fronts, which can be clearly observed in multicolor scale in Fig. 2. Higher-order harmonics will be more affected by the curvature as a result of shorter wavelength. Consequently, the curved wave fronts will lead to the reflected fields being focused at some point in front of the target as propagation. Further, once the focal point is passed, the fields are expected to diverge.

Figures 3(a)–3(d) show the spatial normalized intensity distribution of the 3rd-, 5th-, 7th-, and 9th-order harmonic fields in the $x - y$ ($z = 0$) plane at $t = 8T_0$, respectively. The nth-order harmonic is obtained after spectral filtering by selecting the frequency range of $[n - 0.5, n + 0.5]\omega_0$. Around this time, the fields approximately reach the focal point induced by the curved plasma mirrors, which is close to the target surface due to the large denting curvature. The focal length f_p can be estimated by $\delta_T = w_0^2/2f_p$ to be about $4\lambda_0$ [28], in agreement with the field intensity at $x \approx 36\lambda_0$ in Figs. 2 and 3(a)–3(d). The initial Bessel-Gaussian spatial profile of the driving laser is not observed from the high-order harmonic fields at this stage, because HHG from relativistic plasma mirrors is an extreme nonlinear process which strongly disturbs the field distribution. The spatial and temporal behaviors of the focusing processes are not in phase for different harmonic orders, which may be attributed to numerical dispersion inherent in the finite-difference time-domain (FDTD) method for solving Maxwell's equations in the PIC code [29,30], since the fields experience strong focusing and the resolution is limited in 3D simulations.

After passing the focal point, the fields inevitably tend to diverge. Snapshots of the spatial intensity profile at a later time of $t = 18T_0$ are shown in Figs. 3(e)–3(h). The spatial range of field intensity is significantly enlarged for each harmonic, with considerable energy contained in the wings of the pulses. The high-order harmonic spatial distribution does not exhibit the Bessel-Gaussian feature, same as the early stage.

As further propagation, however, an interesting field profile begins to emerge. The field energy gradually flows from the side lobes towards the middle part and forms a central region with high intensity. As depicted in Figs. 3(i)–3(l), the spatial intensity distribution at $t = 28T_0$ for each harmonic gets focused once again. Different from those at the first focal region caused by the curved plasma mirrors, the redistributed field structures at the second focal region exhibit a main central peak followed by several less intense side lobes. To see the field structure more clearly, we plot the 1D cut field profile in Figs. 3(m)–3(p) along the dashed red lines in Figs. 3(i)–3(l), respectively. It is remarkable that the 1D field distribution for each harmonic order can be well fitted by Bessel functions, indicating the high-order harmonics having been restored to Bessel-Gaussian beams, the same as the driving laser beam, during propagation. In spite of gross deformation due to the extreme nonlinearity and strong defocusing, high-order harmonics in the relativistic optical regime still inherit the

characteristic and capability of self-healing from the fundamental Bessel-Gaussian driving beam. We note that the radial distance between the intensity peaks of the Bessel-Gaussian beams decreases with increasing the harmonic order. This is because the radial electric field of the Bessel beam can also be expressed as $E(r) \propto J_0(k \sin\theta r)$, with θ being the angle of the conic wave composing the Bessel beam to the x axis [24], which is related with the wave vector k and thus the harmonic order n.

Figures 3(q)–3(t) show the unzoomed profiles of the self-healing process for the 3rd-order harmonic. The rings of the Bessel-Gaussian beam are also intense enough to generate high-order harmonics. These harmonics are focused by each curved plasma mirror induced by each of the rings. The focal lengths are a little shorter than that of the central part due to smaller denting parameters as can be seen in Fig. 2. After passing the focal regions, these harmonics also diverge [Fig. 3(r)]. At later times [Figs. 3(s)–3(t)], however, the harmonic energy generated by the rings of the laser pulse is redistributed towards the central region and gradually forms the self-healed Bessel-Gaussian beam. It demonstrates that the self-healing process relies on the low-intensity rings, which behave as reservoirs providing energy redistributed towards the central regions. As a result, the secondary focusing occurs.

To compare the intensity of self-healed Bessel-Gaussian high-order harmonics with that focused by the curved plasma mirrors, we study the peak intensity of attosecond pulses as a function of time and show the evolution results in Figs. 4(a)–4(b) for frequency ranges $n \geqslant 3$ and $n \geqslant 5$, respectively. The intensity reaches the first peak at around $t = 8T_0$ owing to focus by the curved plasma mirrors and then rapidly decreases by an order of magnitude at around $t = 15T_0$ due to diverging after the focus. At a later time, the attosecond pulses gradually recover to Bessel-Gaussian beams so that a second peak is formed at around $t = 23T_0$, with intensity even stronger than that of the first peak by the plasma mirror focusing. Thus, the striking feature of self-healing and associated secondary focusing can be particularly useful for extending the duration of high intensity created by means of relativistic plasma mirrors.

To further demonstrate the advantage of this scheme, we compare the results with those using conventional Gaussian beams. The Gaussian laser also has an amplitude of $a_0 = 15$ and a FWHM pulse duration of $\tau_0 = 5T_0$ with a little larger $1/e^2$ intensity width of $w_e = 2.5\lambda_0$ to ensure the same pulse energy as the Bessel-Gaussian beam. As shown in Figs. 4(a) and 4(b), the high-order harmonics by Gaussian beams also get focused by the curved plasma mirrors at around $t = 8T_0$, with peak intensity slightly higher than that by Bessel-Gaussian beams. However, the intensity by Gaussian beams decreases rapidly and monotonously afterwards, as the fields continuously diverge in the absence of the self-healing property. The peak intensity of attosecond pulses by Bessel-Gaussian beams surpasses that by Gaussian beams by more than 1 order of magnitude and this lasts for tens of laser periods. It should be noted that, in the absence of strong focusing by light pressure, the self-healed Bessel-Gaussian high-order harmonic beam can keep the high intensity propagating for a long time because of the non-diffraction characteristics of Bessel beams.
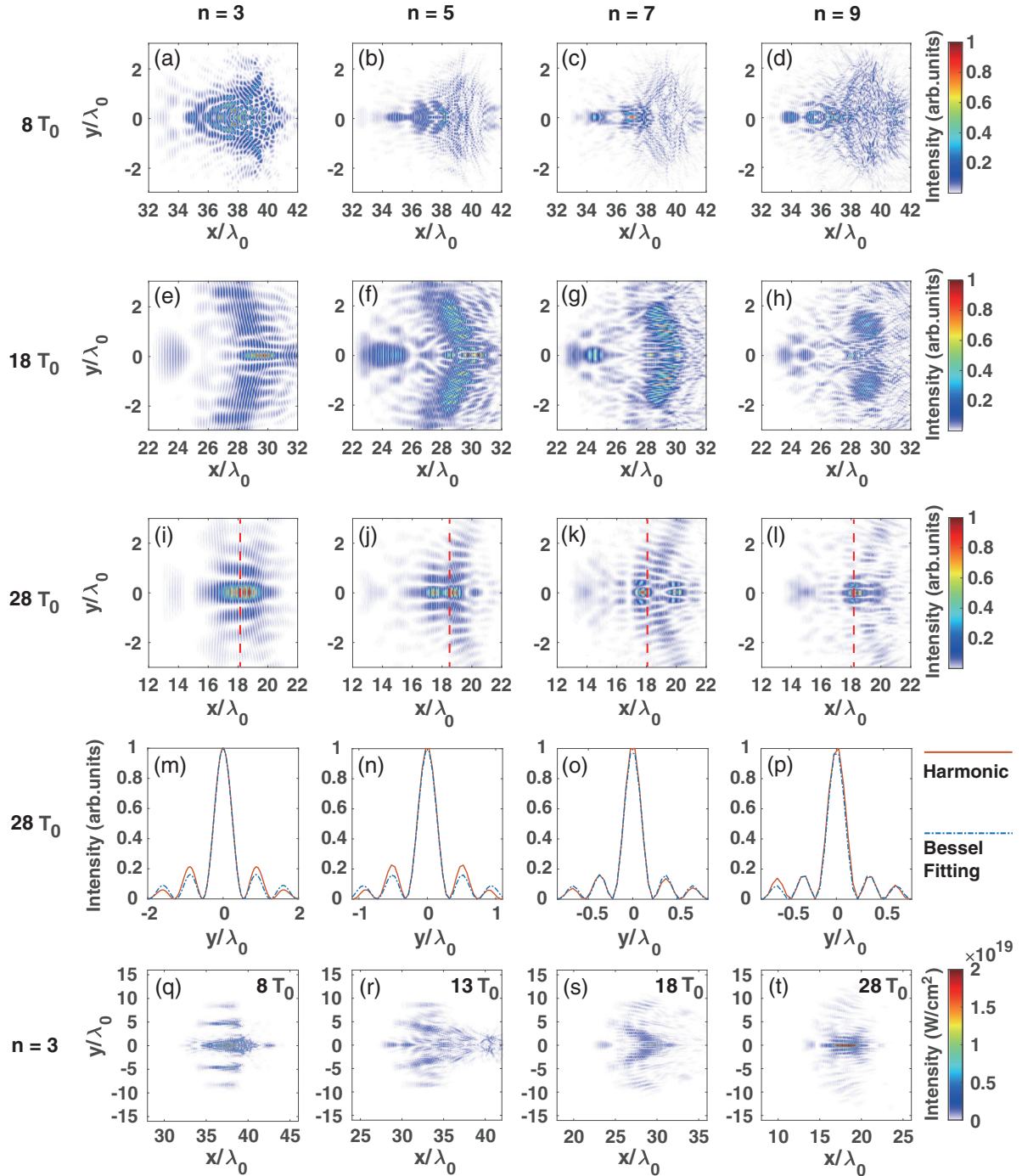
FIG. 3. Self-healing high-order harmonic generation. (a)–(d) Spatial intensity distribution in the $z = 0$ plane at $t = 8T_0$ for the 3rd, 5th, 7th, and 9th harmonic order, respectively. Harmonic intensity distribution corresponding to panels (a)–(d) at (e)–(h) $t = 18T_0$ and (i)–(l) $t = 28T_0$. (m)–(p) 1D cut intensity profile along the dashed red lines in panels (i)–(l), respectively. The dash-dotted blue curves represent fitting by the Bessel function $J_0(0.69yn)$, where n is the harmonic order. (q)–(t) The unzoomed profiles of 3rd-harmonic-order intensity distribution at different times. The intensities are normalized to the peak value in each panel.

Figures 4(c) and 4(d) show snapshots of the 2D spatial intensity profile of the attosecond pulses (harmonic order $n \geqslant 5$) in the $x - y$ plane at $t = 23T_0$ for Gaussian and Bessel-Gaussian beams, respectively. It is evident the pulse intensity by Gaussian beams spreads from the middle over a wide area with relatively low intensity. In contrast, the pulse intensity by Bessel-Gaussian beams converges from the side lobes on the central part. Moreover, the spatial range of high intensity is larger than than by Gaussian beams. Thus the high-intensity region can be extended in both space and time by Bessel-Gaussian beams further than by conventional Gaussian beams, which is highly beneficial for strong-field applications.

In our simulations, the harmonic beam intensities driven by Gaussian and Bessel-Gaussian laser beams are about the same
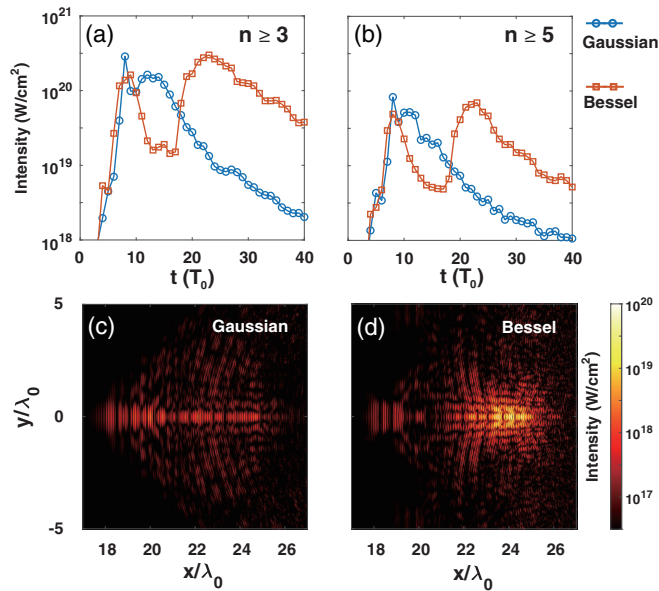
FIG. 4. Comparison of high-order harmonic intensity between Gaussian and Bessel-Gaussian driving beams. Peak harmonic intensity as a function of time for harmonic orders (a) $n \geqslant 3$ and (b) $n \geqslant 5$. A snapshot of 2D spatial intensity distribution for harmonics with order $n \geqslant 5$ in the $z = 0$ plane at $t = 23T_0$ for (c) Gaussian and (d) Bessel-Gaussian driving beams.

level as the driving laser intensity ($I_0 \approx 5 \times 10^{20}$ W/cm^2). The reason for no intensity boost can partly be attributed to the nonoptimal setup, e.g., normal incidence (the self-healing HHG are tested to work at an oblique incidence angle of

15°), and numerical dispersion problems using the FDTD PIC code as mentioned above. However, more accurate 3D PIC simulations using the spectral Maxwell solver have demonstrated that an intensity boost from 10^{22} to 10^{25} W/cm^2 using the curved plasma mirror scheme is possible [11]. In our simulations, $n_0 = 5n_c$ and $a_0 = 15$, giving the similarity parameter $S = n_0/n_ca_0 = 1/3$. According to the relativistic plasma similarity theory [31], similar laser-plasma dynamics can be expected by scaling the parameters, e.g., $a_0 = 600$ ($I_0 \approx 8 \times 10^{23}$ W/cm^2) with $n_e = 200n_c$. The scheme should work in this high-intensity regime, relevant to strong-field QED studies, since the HHG process from relativistic plasma mirrors would not be destroyed by the related QED effects [32].

In summary, we have demonstrated the self-healed generation of Bessel-Gaussian high-order harmonics from plasma mirrors. Compared to high-order harmonics generated by Gaussian-beam-driven curved plasma mirrors, which reach their peak intensity at the focal point of curved plasma mirrors and then rapidly diverge to low intensities, the self-healed Bessel-Gaussian high-order harmonics create a second intensity peak after the focus of curved plasma mirrors, thus considerably extending the high-intensity region in both space and time. The scheme not only is useful for producing bright Bessel-Gaussian beams in the extreme ultraviolet short wavelength range but also can greatly facilitate applications utilizing the extreme fields created by optically curved relativistic plasma mirrors.

[1] U. Teubner and P. Gibbon, High-order harmonics from laser-irradiated plasma surfaces, Rev. Mod. Phys. **81**, 445 (2009).

[2] S. V. Bulanov, N. M. Naumova, and F. Pegoraro, Interaction of an ultrashort, relativistically strong laser pulse with an overdense plasma, Phys. Plasmas **1**, 745 (1994).

[3] R. Lichters, J. Meyer-ter-Vehn, and A. Pukhov, Short-pulse laser harmonics from oscillating plasma surfaces driven at relativistic intensity, Phys. Plasmas **3**, 3425 (1996).

[4] T. Baeva, S. Gordienko, and A. Pukhov, Theory of high-order harmonic generation in relativistic laser interaction with overdense plasma, Phys. Rev. E **74**, 046404 (2006).

[5] B. Dromey, M. Zepf, A. Gopal, K. Lancaster, M. S. Wei, K. Krushelnick, M. Tatarakis, N. Vakakis, S. Moustaizis, R. Kodama, M. Tampo, C. Stoeckl, R. Clarke, H. Habara, D. Neely, S. Karsch, and P. Norreys, High harmonic generation in the relativistic limit, Nat. Phys. **2**, 456 (2006).

[6] B. Dromey, S. Kar, C. Bellei, D. C. Carroll, R. J. Clarke, J. S. Green, S. Kneip, K. Markey, S. R. Nagel, P. T. Simpson, L. Willingale, P. McKenna, D. Neely, Z. Najmudin, K. Krushelnick, P. A. Norreys, and M. Zepf, Bright multi-keV harmonic generation from relativistically oscillating plasma surfaces, Phys. Rev. Lett. **99**, 085001 (2007).

[7] B. Dromey, D. Adams, R. Hörlein, Y. Nomura, S. G. Rykovanov, D. C. Carroll, P. S. Foster, S. Kar, K. Markey, P. McKenna, D. Neely, M. Geissler, G. D. Tsakiris, and M. Zepf, Diffraction-limited performance and focusing of high harmonics from relativistic plasmas, Nat. Phys. **5**, 146 (2009).

[8] S. Gordienko, A. Pukhov, O. Shorokhov, and T. Baeva, Relativistic Doppler effect: Universal spectra and zeptosecond pulses, Phys. Rev. Lett. **93**, 115002 (2004).

[9] S. Gordienko, A. Pukhov, O. Shorokhov, and T. Baeva, Coherent focusing of high harmonics: A new way towards the extreme intensities, Phys. Rev. Lett. **94**, 103903 (2005).

[10] A. A. Gonoskov, A. V. Korzhimanov, A. V. Kim, M. Marklund, and A. M. Sergeev, Ultrarelativistic nanoplasmonics as a route towards extreme-intensity attosecond pulses, Phys. Rev. E **84**, 046403 (2011).

[11] H. Vincenti, Achieving extreme light intensities using optically curved relativistic plasma mirrors, Phys. Rev. Lett. **123**, 105001 (2019).

[12] H. Vincenti, T. Clark, L. Fedeli, P. Martin, A. Sainte-Marie, and N. Zaim, Plasma mirrors as a path to the Schwinger limit: theoretical and numerical developments, Eur. Phys. J. Spec. Top. **232**, 2303 (2023).

[13] F. Quéré and H. Vincenti, Reflecting petawatt lasers off relativistic plasma mirrors: a realistic path to the Schwinger limit, High Power Laser Sci. Eng. **9**, e6 (2021).

[14] M. Marklund, T. G. Blackburn, A. Gonoskov, J. Magnusson, S. S. Bulanov, and A. Ilderton, Towards critical and supercritical electromagnetic fields, High Power Laser Sci. Eng. **11**, e19 (2023).

[15] A. Di Piazza, C. Müller, K. Z. Hatsagortsyan, and C. H. Keitel, Extremely high-intensity laser interactions with fundamental quantum systems, Rev. Mod. Phys. **84**, 1177 (2012).

[16] J. Durnin, J. J. Miceli, and J. H. Eberly, Diffraction-free beams, Phys. Rev. Lett. **58**, 1499 (1987).

[17] D. McGloin and K. Dholakia, Bessel beams: Diffraction in a new light, Contemp. Phys. **46**, 15 (2005).

[18] A. Aiello and G. S. Agarwal, Wave-optics description of self-healing mechanism in Bessel beams, Opt. Lett. **39**, 6819 (2014).

[19] G. Thériault, M. Cottet, A. Castonguay, N. McCarthy, and Y. De Koninck, Extended two-photon microscopy in live samples with Bessel beams: steadier focus, faster volume scans, and simpler stereoscopic imaging, Front. Cell. Neurosci. **8**, 139 (2014).

[20] S. Zhao, W. Zhang, L. Wang, W. Li, L. Gong, W. Cheng, H. Chen, and J. Gruska, Propagation and self-healing properties of Bessel-Gaussian beam carrying orbital angular momentum in an underwater environment, Sci. Rep. **9**, 2025 (2019).

[21] R. Stoian, M. K. Bhuyan, G. Zhang, G. Cheng, R. Meyer, and F. Courvoisier, Ultrafast Bessel beams: advanced tools for laser materials processing, Adv. Opt. Technol. **7**, 165 (2018).

[22] M. Nisoli, E. Priori, G. Sansone, S. Stagira, G. Cerullo, S. De Silvestri, C. Altucci, R. Bruzzese, C. de Lisio, P. Villoresi, L. Poletto, M. Pascolini, and G. Tondello, High-brightness high-order harmonic generation by truncated Bessel beams in the sub-10-fs regime, Phys. Rev. Lett. **88**, 033902 (2002).

[23] A. Pukhov, Three-dimensional electromagnetic relativistic particle-in-cell code VLPL (Virtual Laser Plasma Lab), J. Plasma Phys. **61**, 425 (1999).

[24] F. Gori, G. Guattari, and C. Padovani, Bessel-Gauss beams, Opt. Commun. **64**, 491 (1987).

[25] J. Fortin, G. Rousseau, N. McCarthy, and M. Piche, Generation of quasi-Bessel beams and femtosecond optical X-waves with conical mirrors, Proc. SPIE **4833**, 876 (2003).

[26] K. B. Kuntz, B. Braverman, S. H. Youn, M. Lobino, E. M. Pessina, and A. I. Lvovsky, Spatial and temporal characterization of a Bessel beam produced using a conical mirror, Phys. Rev. A **79**, 043802 (2009).

[27] N. Zaïm, D. Guénot, L. Chopineau, A. Denoeud, O. Lundh, H. Vincenti, F. Quéré, and J. Faure, Interaction of ultraintense radially-polarized laser pulses with plasma mirrors, Phys. Rev. X **10**, 041064 (2020).

[28] H. Vincenti, S. Monchocé, S. Kahaly, G. Bonnaud, Ph. Martin, and F. Quéré, Optical properties of relativistic plasma mirrors, Nat. Commun. **5**, 3403 (2014).

[29] A. Pukhov, X-dispersionless Maxwell solver for plasma-based particle acceleration, J. Comput. Phys. **418**, 109622 (2020).

[30] G. Blaclard, H. Vincenti, R. Lehe, and J. L. Vay, Pseudospectral Maxwell solvers for an accurate modeling of Doppler harmonic generation on plasma mirrors with particle-in-cell codes, Phys. Rev. E **96**, 033305 (2017).

[31] S. Gordienko and A. Pukhov, Scalings for ultrarelativistic laser plasmas and quasimonoenergetic electrons, Phys. Plasmas **12**, 043109 (2005).

[32] S. Hu and Z.-Y. Chen, QED effects on high-order harmonic generation from ultraintense laser-irradiated solid-plasmas, Phys. Plasmas **29**, 013102 (2022).